Geomorphology xxx (2015) xxx–xxx

Contents lists available at ScienceDirect

Geomorphology

journal homepage: www.elsevier.com/locate/geomorph

The Landscape Evolution Observatory: A large-scale controllable infrastructure to study coupled Earth-surface processes

Luke A. Pangle [a,*], Stephen B. DeLong [a,b], Nate Abramson [a], John Adams [a], Greg A. Barron-Gafford [a,c], David D. Breshears [d,i], Paul D. Brooks [p], Jon Chorover [f], William E. Dietrich [g], Katerina Dontsova [a], Matej Durcik [a], Javier Espeleta [a,h], T.P.A. Ferre [e], Regis Ferriere [i,q], Whitney Henderson [a], Edward A. Hunt [a], Travis E. Huxman [j], David Millar [a], Brendan Murphy [a,k], Guo-Yue Niu [a,e], Mitch Pavao-Zuckerman [a], Jon D. Pelletier [l], Craig Rasmussen [f], Joaquin Ruiz [a,l,m], Scott Saleska [i], Marcel Schaap [f], Michael Sibayan [a], Peter A. Troch [a,e], Markus Tuller [f], Joost van Haren [a,n], Xubin Zeng [o]

[a] Biosphere 2, University of Arizona, Tucson, AZ 85738, USA
[b] United States Geological Survey, Menlo Park, CA 94025, USA
[c] School of Geography and Development, University of Arizona, Tucson, AZ 85721, USA
[d] School of Natural Resources and the Environment, University of Arizona, Tucson, AZ 85721, USA
[e] Department of Hydrology and Water Resources, University of Arizona, Tucson, AZ 85721, USA
[f] Department of Soil, Water and Environmental Science, University of Arizona, Tucson, AZ 85720, USA
[g] Department of Earth and Planetary Science, University of California at Berkeley, Berkeley, CA 94720, USA
[h] Department of Civil and Environmental Engineering, University of Washington, Seattle, WA 98195, USA
[i] Department of Ecology and Evolutionary Biology, University of Arizona, Tucson, AZ 85721, USA
[j] Center for Environmental Biology, University of California at Irvine, Irvine, CA 92697, USA
[k] Jackson School of Geosciences, University of Texas, Austin, TX 78712, USA
[l] Department of Geosciences, University of Arizona, Tucson, AZ 85721, USA
[m] College of Science, University of Arizona, Tucson, AZ 85721, USA
[n] Honors College, University of Arizona, Tucson, AZ 85721, USA
[o] Department of Atmospheric Sciences, University of Arizona, Tucson, AZ 85721, USA
[p] Department of Geology and Geophysics, University of Utah, Salt Lake City, UT 84112, USA
[q] IBENS, Eco-evolutionary Mathematics Group, CNRS UMR 8197, Ecole Normale Superieure, 46 rue d'Ulm, 75005 Paris, France

ARTICLE INFO

Article history:
Received 30 May 2014
Received in revised form 16 January 2015
Accepted 21 January 2015
Available online xxxx

Keywords:
Zero-order basin
Water cycle
Carbon cycle
Energy balance
Soil weathering
Coevolution

ABSTRACT

Zero-order drainage basins, and their constituent hillslopes, are the fundamental geomorphic unit comprising much of Earth's uplands. The convergent topography of these landscapes generates spatially variable substrate and moisture content, facilitating biological diversity and influencing how the landscape filters precipitation and sequesters atmospheric carbon dioxide. In light of these significant ecosystem services, refining our understanding of how these functions are affected by landscape evolution, weather variability, and long-term climate change is imperative. In this paper we introduce the Landscape Evolution Observatory (LEO): a large-scale controllable infrastructure consisting of three replicated artificial landscapes (each 330 m^2 surface area) within the climate-controlled Biosphere 2 facility in Arizona, USA. At LEO, experimental manipulation of rainfall, air temperature, relative humidity, and wind speed are possible at unprecedented scale. The Landscape Evolution Observatory was designed as a community resource to advance understanding of how topography, physical and chemical properties of soil, and biological communities coevolve, and how this coevolution affects water, carbon, and energy cycles at multiple spatial scales. With well-defined boundary conditions and an extensive network of sensors and samplers, LEO enables an iterative scientific approach that includes numerical model development and virtual experimentation, physical experimentation, data analysis, and model refinement. We plan to engage the broader scientific community through public dissemination of data from LEO, collaborative experimental design, and community-based model development.

1. Introduction

Hillslopes and their adjacent hollows (i.e., zero-order drainage basins, or ZOBs) constitute a large fraction of upland areas over Earth's

* Corresponding author at: PO Box 8746, Biosphere 2, University of Arizona, Tucson, AZ 85738, USA.
E-mail address: lpangle@email.arizona.edu (L.A. Pangle).

http://dx.doi.org/10.1016/j.geomorph.2015.01.020
0169-555X/

surface and provide critical ecosystem services. Within ZOBs there is exchange of water, carbon dioxide, and energy with the atmosphere and transport of soil, water, and solutes into fluvial drainage networks—processes that link ZOBs with the climate system and downstream water quantity and quality. The time-varying rates of these exchanges and transport processes are integrated responses to many physical and biological phenomena that occur from below the base of the soil profile to the vertical extent of the atmospheric boundary layer (e.g., see discussion by Chorover et al., 2011).

Zero-order basins evolve as climate varies, soils form and erode, and biological communities establish, compete, and change in response to environmental stimuli. Across spatial and topographic gradients, these interacting processes may result in consistently observable correlations between temperature and precipitation dynamics, soil depth and hillslope length, and plant biomass accumulation (e.g., Rasmussen et al., 2011; Pelletier et al., 2013). Coupled soil-production and soil-transport models give us the ability to make process-based predictions about the spatial variation of soil depth, which is typically thin and relatively static on ridges and gradually thickening in convergence areas and valley bottoms (e.g., Dietrich et al., 1995). The covarying physical attributes of landscapes and the biological communities that inhabit them are shown to correlate well with some of the storage and flux components of their water, biogeochemical, and energy cycles, for example, the way they store and transmit water to streams (e.g., Ali et al., 2012a,b; Troch et al., 2013). A fundamental goal of interdisciplinary Earth science remains to understand the mechanistic links between geomorphological processes, physical and chemical evolution of soils, biological community dynamics, and the cycling of water, carbon, and energy.

Zero-order basins and their constituent hillslopes are often chosen as units of study in investigations of geomorphological and hydrological processes (e.g., Dietrich et al., 1987; Wilson and Dietrich, 1987; Dietrich et al., 1992; Sidle et al., 2000; van Tol et al., 2010a,b; Bachmair and Weiler, 2012; Bachmair et al., 2012). These landscapes are advantageous for process-based studies because they exhibit significant spatial variability in slope angle, aspect, soil properties, net radiation, hydraulic gradients, biological community composition, and biogeochemical processes over relatively small land areas. In some cases, their spatial scale enables analyses of how point- to plot-scale processes influence integrated fluxes of mass and energy at the whole-ZOB scale. However, working at the spatial scale of ZOBs also imposes profound methodological challenges. Controlled and replicated experimentation at this scale — where experimental variables can be manipulated rather than only observed — is expensive, logistically daunting, and therefore rare.

Combining controlled experimentation with observational studies and numerical modeling is an effective approach to advancing our knowledge of landscape evolution and how that evolution influences the cycling of mass and energy between the land and atmosphere (e.g., Norby and Luo, 2004; Osmond et al., 2004; Niemann and Hasbargen, 2005; Kleinhans et al., 2010). Below we briefly describe some specific challenges that hinder controlled experimentation in field-based studies of coupled geomorphological, hydrological, and biological processes at the ZOB scale. We then introduce the Landscape Evolution Observatory — a new scientific infrastructure that addresses these challenges. The remaining sections of the paper provide detailed descriptions of the facility, the manipulative and measurement capabilities, and an operational plan that incorporates the broader scientific community through planning workshops, data dissemination, and opportunities for collaborative research.

1.1. Challenges to controlled-experimental research in open environmental systems

A major limitation to experimental research of landscape evolution processes is the difficulty of developing replicated experimental designs involving hillslopes and ZOBs. A tenet of experimental design is the identification of *experimental units* (e.g., individual organisms and field plots) that can be logically categorized into groups with specific and consistent attributes relative to the experiment (e.g., by species and topographic position) and can have one or more experimental manipulations imposed upon them either randomly or systematically [e.g., see discussions by Hurlbert (1984) and Jenerette and Shen (2012)]. Through replication, one can quantify variability that exists within groups of experimental units receiving different manipulations. The magnitude of the effect of an experimental manipulation can then be evaluated statistically, to determine whether it caused a deviation in the response variable that is greater than the inherent variability among experimental units. In addition to the logistical challenges associated with replicated experiments and measurements at the ZOB scale, there is the more fundamental problem of logically grouping ZOBs based on similarities and differences. If subsurface water flow was the response variable of interest, for example, it may be strongly influenced by the geometry and connectivity of soil-macropore networks (e.g., Zehe and Fluhler, 2001), the spatial organization of soil types (e.g., van Tol et al., 2010b), or the topography and local conductivity of the underlying bedrock (e.g., Montgomery et al., 1997; Freer et al., 2002). These landscape features are extremely difficult to observe and quantify over large land areas and therefore are used rarely for grouping hillslopes and ZOBs within replicated experimental designs.

A second important challenge to experimental work in ZOBs is the inability to manipulate experimental variables. Infrequent and transient climate events, such as very large storms, can trigger threshold-based erosion processes (e.g., see discussion by Phillips, 2003) and the formation of water-flow path networks (e.g., McGrath et al., 2007; Zehe and Sivapalan, 2009) that persist over long periods of time. These events may also facilitate persistent changes in the spatial organization of biological communities and soil physical and chemical properties (e.g., Saco et al., 2007; Stavi et al., 2009). Severe droughts can also have long-lasting impacts on plant-community composition (e.g., Adams et al., 2009). We typically lack knowledge about the historical occurrence of such climate events within specific ZOBs, and because of their infrequency we have limited opportunities to observe and analyze their short- and long-term impacts. The ability to perform repeated manipulations of precipitation would help answer questions regarding what precipitation intensities, durations, or sequence of pulses cause spatial differentiation in soil physical and chemical properties, water-flow path development, and the composition of microbial and vascular plant communities.

A third challenge to experimental investigations of landscape evolution processes is the inability to monitor multiple physical and biological response variables at high spatial and temporal resolution. This is especially true when the response variables are continuous in space (e.g., soil-water content or vapor-pressure deficit throughout plant canopies) and occur below the soil surface (e.g., root growth and rhizosphere chemistry). The evolution of landscapes results from processes occurring across orders of magnitude in scale; from biogeochemical reactions at the interface between soil water and soil particles (e.g., Chorover et al., 2007) to the development of water-flow networks and plant community organization across square meters to square kilometers (e.g., Thompson et al., 2010, 2011). Typical measurement scales for many important variables are on the order of cubic centimeters, making extrapolation across landscapes unreliable. What is needed, though expensive and difficult to organize, are collocated measurements of physical, chemical, and biological state and flux variables at high spatial resolution and across broad areas — and interdisciplinary teams of scientists to interpret their meaning.

Measurement limitations also hinder our ability to learn through the use of numerical models. Numerical modeling and virtual experiments can be used to inform hypotheses, guide the planning of field and laboratory studies, and strengthen mechanistic understanding of laboratory and field data. Numerical models are exceptionally useful in that they can simulate many different experimental scenarios, processes, and interactions between variables (at least simplified conceptions of them)

Please cite this article as: Pangle, L.A., et al., The Landscape Evolution Observatory: A large-scale controllable infrastructure to study coupled Earth-surface processes, Geomorphology (2015), http://dx.doi.org/10.1016/j.geomorph.2015.01.020

at potentially high spatial and temporal resolution. Despite these advantages, available data are rarely sufficient to test rigorously the model assumptions or constrain the many parameters that are intended to reflect real properties of the study system (e.g., Kirchner, 2006; Vache and McDonnell, 2006; Fenicia et al., 2008; Clark et al., 2011; Beven, 2012). To improve our learning from numerical models we must test them against high resolution data sets representing multiple state and flux variables in systems subject to known climate forcing and initial conditions. Such data sets are rare at the ZOB scale.

1.2. The Landscape Evolution Observatory: an innovative new tool to advance experimental investigations of coupled Earth-surface processes

In this paper we introduce the Landscape Evolution Observatory (LEO) — a new large-scale research infrastructure consisting of three artificial landscapes (330 m^2 surface area; 330 m^3 volume; 10° average slope) that emulate ZOBs. The landscapes are located inside a climate-controlled glass house that is part of the Biosphere 2 facility in Arizona, USA. The landscapes are designed as experimental replicates: their physical dimensions are nearly identical and the same crushed rock was used as parent material. Experimental variables that can be manipulated individually, or in combination, include precipitation amount and chemistry, air temperature, relative humidity, and wind speed. The eventual introduction of vegetation (discussed in Section 8) also represents a manipulative-experimental capability (e.g., species composition and planting density).

LEO was conceived as a long-term experiment that would enable intensive monitoring of energy, water, and carbon cycles; the chemical and physical evolution of soil; and the changing morphology of the landscape surface starting from an initial condition of spatially uniform crushed rock. We describe this infrastructure using the word *observatory* to convey that this specific apparatus can be used in an iterative process with field experiments in the real world, smaller scale laboratory experiments in highly controlled settings, and numerical models that simulate coupled Earth-surface processes. The word *observatory* therefore reflects the open nature of the facility and the opportunities for different modes of collaborative experimentation, monitoring, and modeling that collectively lead to new knowledge. A multiyear planning process involving University of Arizona scientists and the broader scientific community (Dontsova et al., 2009; Hopp et al., 2009; Huxman et al., 2009; Ivanov et al., 2010) led to the construction phase from 2010 through 2012. Some fundamental questions that motivated LEO include:

- How does variability in climate and the physiological function of microbial and vascular plant communities control the rate of physical and chemical transformation of rock to soil?
- How does the physical and chemical transformation of soil, and the evolution of landscape morphology, control spatial and temporal trends in soil moisture and the formation of water-flow path networks?
- How do vascular plant communities organize in response to landscape evolution processes, and through what mechanisms do they exert control over erosive processes and the changing topography of the land surface?
- Can we synthesize research findings from LEO into improved numerical models that more accurately simulate landscape evolution processes and the coupled exchange of energy, water, and carbon between the land and atmosphere?

These research questions are similar to those that motivated other networks of large-scale field observatories and experiments, like the Critical Zone Observatories (e.g., Brantley et al., 2007; Dybas, 2013), the FLUXNET network, and the Free-Air CO_2 Enrichment (FACE) experiments (e.g., Norby and Zak, 2011). However, in terms of spatial scale, topographic complexity, climate control, and monitoring capabilities, LEO is distinct from and complimentary to those observatories and other prior field and laboratory studies (Fig. 1; see Osmond et al., 2004).

The Landscape Evolution Observatory is the world's largest controlled laboratory experiment focusing on coupled Earth-surface processes within a multiyear period of closely monitored landscape evolution. Initial research at LEO will focus on interactions between hydrological and geochemical processes in the absence of vegetation and significant topographic evolution. Anticipated landscape evolution processes during this time include changes in microtopographic roughness caused by raindrop splash (e.g., Dunne et al., 2010) and incipient physical and chemical weathering of the parent material (Dontsova et al., 2009). The eventual establishment of plants on the LEO landscapes is anticipated to profoundly influence soil chemistry and structure (e.g., Angers and Caron, 1998), local infiltration rates (e.g., Thompson et al., 2010), hydrological connectivity of the surface (e.g., Bromley et al., 1997), sediment transport, and topographic evolution (e.g., Harman et al., 2014).

Whereas climate variables are uncontrollable in large-scale field studies, at LEO it is possible to prescribe specific sequences of precipitation intensity and duration, seasonally wet and dry periods, variable temperature, humidity, and wind velocity. With more than 1700 sensors and sampling devices installed within each landscape, LEO provides unparalleled capabilities to monitor co-occurring geomorphological, hydrological, and biogeochemical processes. Those spatially resolved measurements are coupled with closed-system mass-balance methods for quantifying total energy, water, and carbon budgets at the whole-landscape scale.

The LEO landscapes were designed to be as nearly identical as possible, but with some inevitable differences caused by, for example, differences in soil packing. Replication of landscapes enables quantification of variability in response metrics, which is essential for statistical hypothesis testing (e.g., see discussion by Underwood, 1993) and for identifying plausible ranges of model parameters and simulation results. More fundamentally, replication makes it possible to observe the repeatability of results — a tenet of scientific research. The LEO landscapes are large enough, and have sufficient topographic relief, that sources of landscape heterogeneity (e.g., surface/subsurface flow networks and biological community organization) are anticipated to emerge across spatial scales ranging from the soil pore to the hillslope. Even upon nearly identical model landscapes exposed to the same climate, will these sources of landscape heterogeneity evolve synchronously, demonstrate similar geometric patterns, and have similar impacts on whole-landscape mass and energy cycles? We contend that these questions cannot be answered a priori, and therefore require treatment and observation of the LEO landscapes as experimental replicates.

LEO enables a scientific approach that includes rapid iterations of hypothesis generation, numerical-model development and simulation, physical experimentation, and learning through data analysis and model revision. The data generated at LEO can be used to evaluate model assumptions and parameterization schemes more rigorously than has been achieved to date. As such, LEO will serve as a tool that can be used collaboratively by experimentalists and modelers representing multiple Earth science disciplines.

2. The Landscape Evolution Observatory: a large-scale controllable infrastructure consisting of replicated physical models of a zero-order basin

LEO includes replicated ($n = 3$) artificial landscapes that were constructed to emulate the topography of a zero-order basin (Figs. 2 and 3). The landscapes are supported by steel structures that are located within an ≈2000-m^2 glass-walled space-frame structure that is part of the Biosphere 2 facility near Oracle, AZ (Fig. 2). The two-dimensional area of each trough is 330 m^2 (30 m × 11 m). The interior of the base

Please cite this article as: Pangle, L.A., et al., The Landscape Evolution Observatory: A large-scale controllable infrastructure to study coupled Earth-surface processes, Geomorphology (2015), http://dx.doi.org/10.1016/j.geomorph.2015.01.020

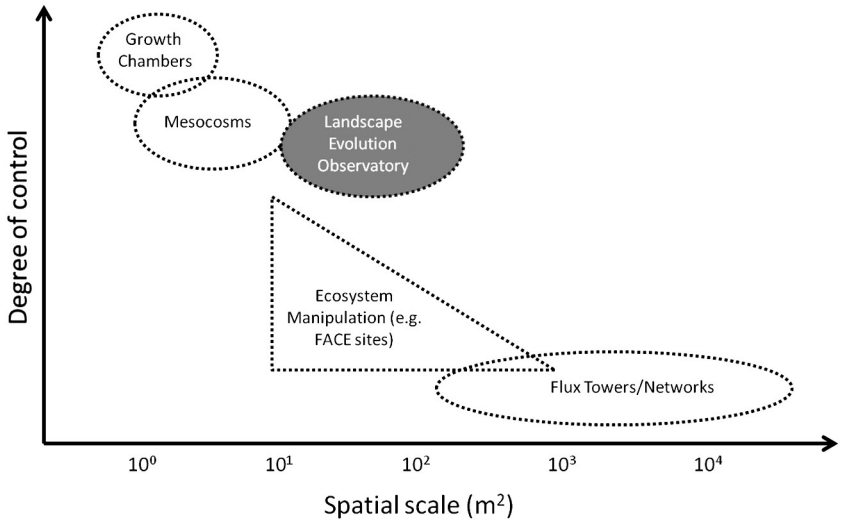

Fig. 1. Schematic diagram comparing spatial scale (m^2) and relative degree of control achieved within different experimental systems in laboratory and field settings.

of each trough was covered with concrete board, then coated with Duraldeck two-part epoxy primer, an elastomeric two-part urethane membrane, and an aggregate-filled aliphatic urethane topcoat (Euclid Chemical Company), yielding a water tight and impermeable boundary at the base of the soil profile (described below).

Each trough was filled with 330 m^3 of ground basaltic tephra with a loamy sand texture (Fig. 5, Table 1) to nearly uniform 1-m depth across the landscape (Figs. 3 and 4). The complete mineral and elemental composition of the basalt is shown below.

Glass	$Ca_{0.44}Mg_{0.30}Na_{0.26}K_{0.06}Mn_{0.01}Fe_{0.38}Al_{0.62}Ti_{0.07}(HPO_4)_{0.03}Si_{1.80}O_{5.87}$
Labradorite	$Ca_{0.69}Mg_{0.01}Fe_{0.04}Na_{0.3}K_{0.01}Al_{1.64}Si_{2.32}O_8$
Forsterite	$Mg_{1.64}Ca_{0.01}Fe_{0.33}SiO_4$
Diopside	$Ca_{0.86}Mn_{0.01}Mg_{0.78}Na_{0.03}Ti_{0.05}Al_{0.22}Fe_{0.27}Cr_{0.01}Si_{1.81}O_6$
Titanomagnetite	$Fe_{2.31}Mg_{0.26}Ca_{0.02}Mn_{0.02}Cr_{0.01}Al_{0.18}Ti_{0.49}Si_{0.06}O_4$

The original rock material was extracted from a >30-m-thick deposit of late Pleistocene airfall tephra associated with Merriam Crater in northern Arizona. The material was installed onto the landscapes via conveyor-belt lifts and wheel barrows in 0.32-m-thick layers. Each layer was then compacted to a thickness of 0.25 m using a pneumatic tamping device that was passed uniformly over the entire landscape. This methodology resulted in a total material depth of 1 m (with some small scale variation; Fig. 3) and a dry bulk density of ≈ 1.5 g cm^{-3} (i.e., ≈ 500 metric tons of crushed basalt per landscape).

Though the material depth is approximately 1 m throughout (based on laser scans performed before and after filling the structures with crushed basalt), the geometry of the underlying steel structure conveys a convergent topographic shape to the overlying soil, with two small upslope troughs merging to form a larger downslope convergent zone with opposing east- and west-facing hillslope facets (Fig. 3). The

Fig. 2. A photograph of one LEO landscape. Pictured is Dr. Steve DeLong. (inset). A wide-angle photograph of the three climate-controlled bays at Biosphere 2 within which the LEO landscapes are contained, and one of the steel structures that support the LEO landscapes — viewed from the floor space within the LEO facility.
Photographs credited to Paul Ingram.

Please cite this article as: Pangle, L.A., et al., The Landscape Evolution Observatory: A large-scale controllable infrastructure to study coupled Earth-surface processes, Geomorphology (2015), http://dx.doi.org/10.1016/j.geomorph.2015.01.020

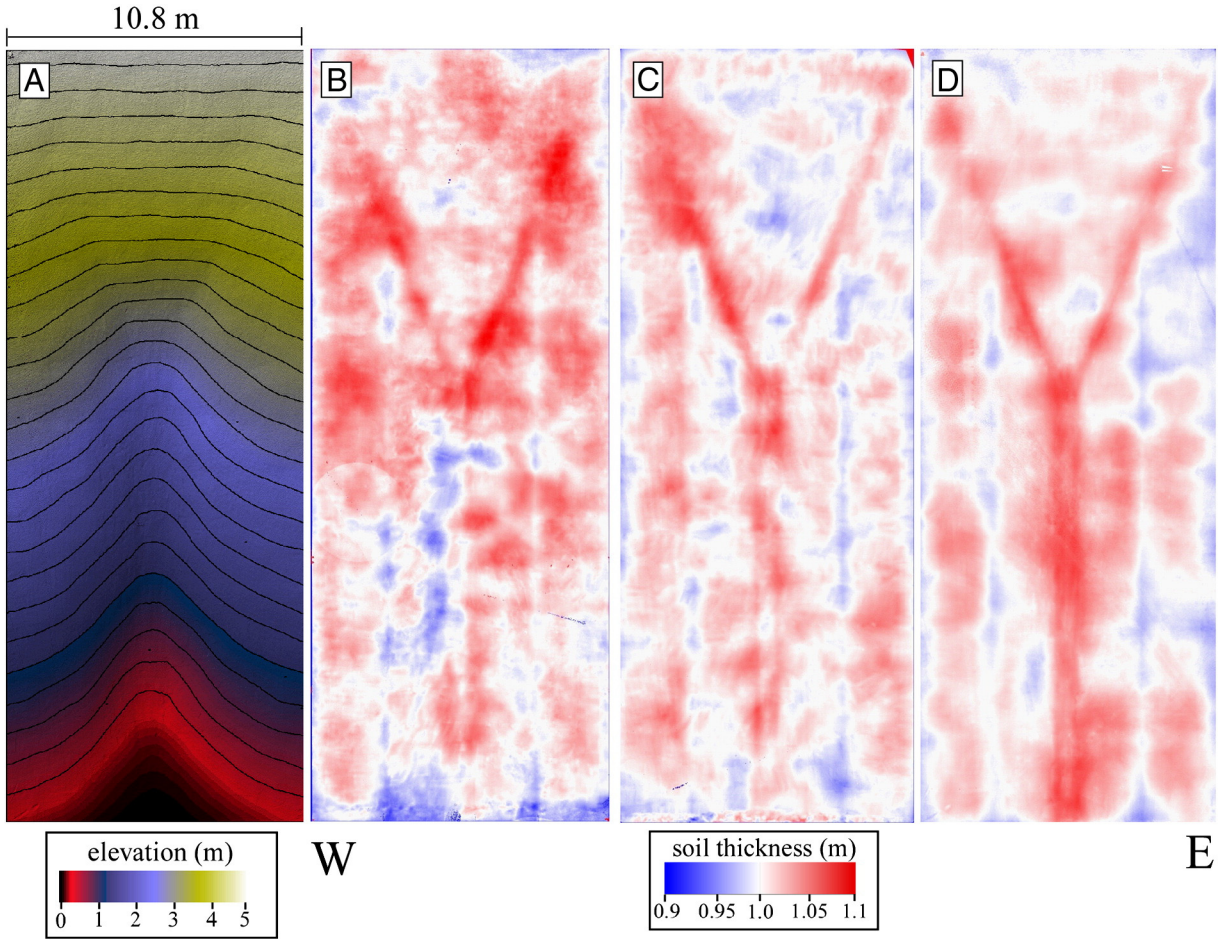

Fig. 3. (A) A shaded-relief map (0.2-m contour line intervals; illumination direction from the upper left) of a digital elevation model of one of the LEO landscapes — measured with a terrestrial laser scanner. (B–D) Shaded contour plots illustrating horizontal variability in total soil depth (m) for the western (B), center (C), and eastern (D) LEO landscapes. The soil depths were derived based on laser scans of the underlying steel structure prior to filling with soil, and laser scans performed after the soil was filled and packed into the structure.

average slope of each landscape is 10°, though the local slope varies from upslope positions into the convergence zones, with maximum slope of 17° near the convergence zone. The valley axis of each convergence zone forks in the upper one-third of the landscape, with the two shallow troughs separated by a planar slope (Fig. 3). This is common in ZOBs in nature (e.g., Dietrich et al., 1987).

The crushed basalt was chosen not to represent a specific landscape within any particular geographic region, and the LEO landscapes were not designed to precisely emulate the sequential transformation of solid rock to soil — a continuous process that spans millennia. The initial depth, physical and chemical uniformity, and specific surface area of the crushed basalt are different than would be observed during soil formation in nature. Other factors such as faunal activity, aeolian erosion, and freeze–thaw cycles are also excluded from the experimental design. Rather, LEO was designed to investigate the coevolution of soil and landscape complexity and associated effects on mass and energy cycles, as influenced by interacting biological, chemical, and physical processes. Because of the initial spatial uniformity and purely mineral composition of the crushed basalt, the biogeochemical and morphological evolution of soil can be observed and quantified beginning from a well-defined initial condition. The depth and texture of the crushed basalt makes possible the introduction of a broader range of plant functional types, from surface-dwelling algae to woody-stemmed vascular plants; and the texture is anticipated to facilitate significant weathering within an observational period of several years.

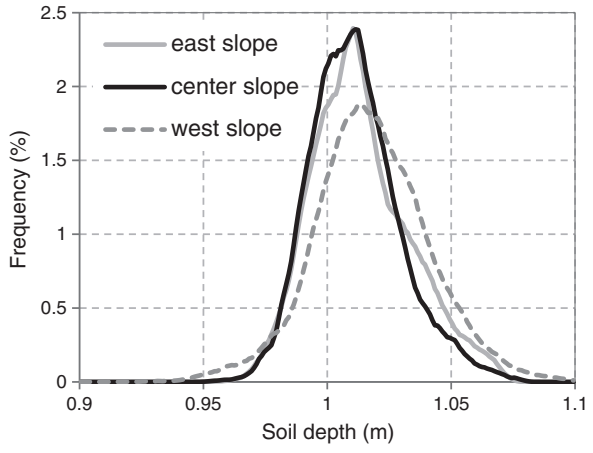

Fig. 4. Frequency distribution of soil depths (m) measured on each LEO landscape. The soil depths were derived based on the same laser scans described in Fig. 3.

The prospective hydraulic properties and biogeochemical weathering rates of multiple materials were considered in preliminary modeling studies conducted during the project design phase (Dontsova et al., 2009; Hopp et al., 2009; Ivanov et al., 2010) — studies that were guided by workshops that engaged the broader research community. The ground basaltic tephra was chosen to represent the parent material of each landscape based on several design criteria that emerged from those workshops, including (i) projected hydraulic properties that would enable sufficient water-storage capacity to support the growth of microbes and vascular plants, (ii) hydraulic conductivity that would be sufficiently great to facilitate regular subsurface flow for the purpose

Please cite this article as: Pangle, L.A., et al., The Landscape Evolution Observatory: A large-scale controllable infrastructure to study coupled Earth-surface processes, Geomorphology (2015), http://dx.doi.org/10.1016/j.geomorph.2015.01.020

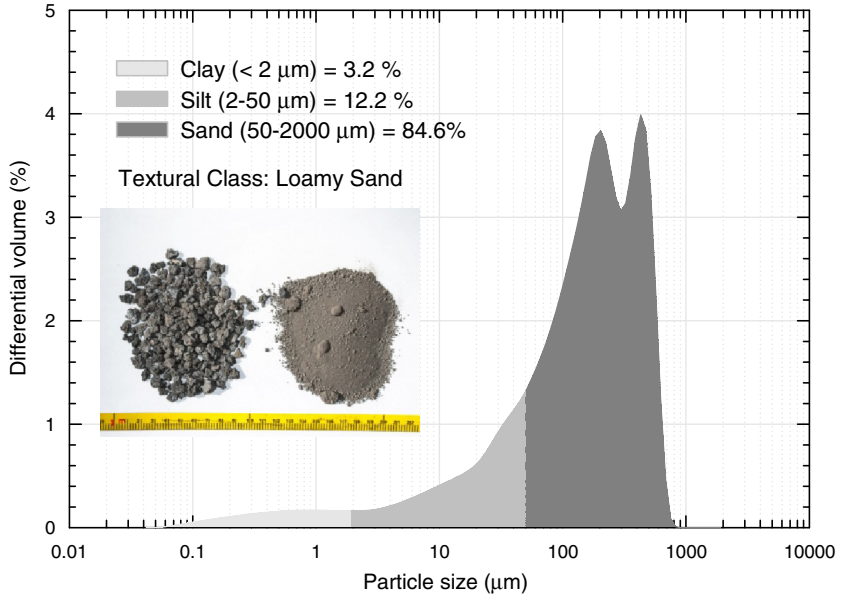

Fig. 5. Particle-size distribution of the ground basalt that fills each LEO landscape. The particle-size distribution was measured via the laser diffraction method using a Beckman Coulter LS 13 320 at the Center for Environmental Physics and Mineralogy, University of Arizona. The legend entries include the cumulative fraction of particles that are categorized as clay, silt, or sand. The inset photo illustrates the basaltic tephra before and after grinding. The textural class (based on the USDA soil texture classification system) is loamy sand and the particle sizes associated with the 10th, 50th, and 90th percentiles of the cumulative particle-size distribution are 13, 162, and 464 μm, respectively. The specific surface area of the crushed basalt is 0.92 $m^2\ g^{-1}$, measured via nitrogen gas adsorption.

of studying flow and mass transport out of the landscape, (iii) hydraulic conductivity that was not so high to prevent the formation of localized heterogeneity in water-table formation and soil moisture dynamics across the landscape, (iv) the projected weathering rates of the basalt tephra were sufficiently great that significant amounts of secondary minerals and clay particles would form during the anticipated 10-year lifespan of the experiment, and (v) the primary elemental composition of the basalt tephra (Dontsova et al., 2009) included phosphorus that, upon weathering, would provide a critical nutrient for colonizing vascular plants. The hydraulic properties analyzed by Hopp et al. (2009) were derived based on empirical relationships with soil textural properties. Subsequent laboratory measurements of the moisture-retention characteristic of the crushed basalt were performed at the University of Arizona (Fig. 6). These measurements were performed on 10 core samples using Tempe Pressure Cells (Soil Moisture Corp.) and an air compressor. The water pressure associated with a volumetric water content of 0.01 was determined using a WP4 Dewpoint Potentiometer (Decagon Devices, Inc.).

3. Climate control and monitoring of the surface energy balance at LEO

The LEO landscapes are located inside three adjacent bays within the southwestern section of Biosphere 2 (Fig. 2) and separated by air partitioning structures. The exterior walls of Biosphere 2 are comprised of 0.011-m-thick duo-laminated glass with an interior Mylar sheet and are supported by latticed space frame construction (Fig. 2). The laminated glass has a solar-heat-gain coefficient of 0.7 and directly transmits 50–60% of solar radiation, yet <1% of ultraviolet radiation. The transmission ratios for varying wavelengths were shown in previous works at Biosphere 2 (Finn, 1996; Marino et al., 1999). Further spectral measurements show that the glass walls cause a small increase in diffuse radiation relative to ambient conditions outside of the structure (Dr. Joost van Haren, University of Arizona, personal communication, 2014).

Temperature and relative humidity are controlled independently within each bay. Air circulation within each bay is driven by three air-handler systems (26 $m^3\ s^{-1}$ flow capacity; two with 40 kW motored fans and one with a 60 kW motored fan) through a duct system such

Table 1
The mean and standard deviation of nitrogen and carbon content (top; $n = 3$) and the fractional mineral composition (bottom; $n = 2$) of the ground basalt that fills each LEO landscape.

	Mean (g/g)	Standard deviation (g/g)
Total nitrogen	4.33×10^{-6}	1.53×10^{-6}
Total carbon	9.33×10^{-5}	1.61×10^{-5}
Inorganic carbon	2.30×10^{-5}	1.73×10^{-6}
Organic carbon	7.03×10^{-5}	1.63×10^{-5}
Glass	0.578	0.0254
Labradorite	0.234	0.0212
Forsterite	0.126	0.00566
Diopside	0.0530	0.0184
Titanomagnetite	0.0100	0.0141

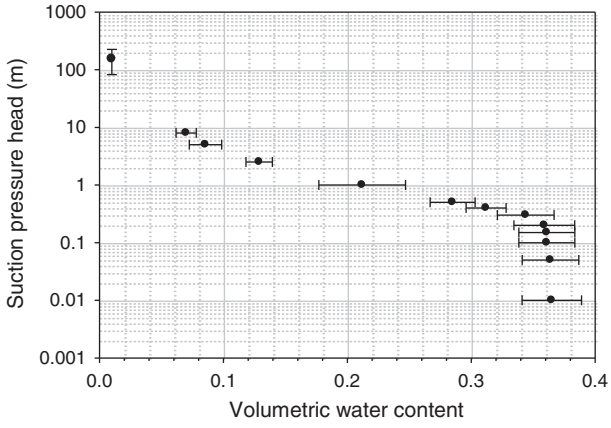

Fig. 6. Moisture retention curves for the crushed basalt used as parent material in the LEO landscapes. Measurements were performed on 10 soil cores extracted from a 208-L barrel within which the crushed basalt was packed to a bulk density of 1.59 g cm^{-3} (standard deviation among cores was 0.13 g cm^{-3}) and exposed to wetting and drying cycles. Horizontal error bars indicate the standard deviation in volumetric water content among the replicate cores at each level of pressure. The data point corresponding to a volumetric water content of 0.01 has vertical error bars that indicate the standard deviation in pressure head observed among the 10 cores at that water content.

Please cite this article as: Pangle, L.A., et al., The Landscape Evolution Observatory: A large-scale controllable infrastructure to study coupled Earth-surface processes, Geomorphology (2015), http://dx.doi.org/10.1016/j.geomorph.2015.01.020

that the prevailing flow of air moves down the long-axis of the landscapes, from the upper slope to the lower slope position (see floor plans in Marino et al., 1999). The air-handlers contain coiled radiators that circulate variably heated or cooled water that is generated from boiler/chiller units and/or an evaporatively cooled water tower. The system can be operated automatically via proportional-integral-derivative (PID) controllers, enabling real-time control of temperature and relative humidity within the LEO atmosphere.

An array of environmental sensors enables monitoring of the surface-energy balance at the LEO landscapes, with the net radiation at the soil surface written as

$$R_n = H + \lambda ET + G \quad (1)$$

where R_n is net radiation; H represents sensible heat flux; λET represents latent heat flux as the product of the latent heat of vaporization (λ) and evaporative loss of water mass from the landscape (ET); G is the heat conduction into the soil, and all variables are functions of time (we note that the *aboveground* instrumentation described in this section was installed over one LEO landscape during the spring of 2014; the same instruments and vertically hanging masts will be installed over the other two slopes during the winter/spring of 2014/2015).

Five vertical masts are attached to the Biosphere 2 space frame above the LEO landscapes. Incident visible light (Apogee Instruments Quantum Sensor), temperature and relative humidity (HMP-60 sensors, Vaisala, Inc.), and wind speed (Standard Cup Anemometer, Davis Instruments) are measured at five locations along each mast: 0.25, 1, 3, 6, and 9–10 m above the soil surface (Fig. 7). Two of the masts (those overlying the east and west facing slope segments; see Fig. 7) are also equipped with four-way net radiometers (CNR4 Net Radiometers, Kipp & Zonen B.V.) that measure incoming and outgoing short- and long-wave radiation. The evaporative loss of water from the landscapes is monitored via mass-balance calculations and atmospheric measurements (detailed in Section 4), and the heat flux into the soil is measured at 24 locations — arranged in a regular grid — by Huskeflux HPF-1 and HPF-1SC surface heat-flux plates (Fig. 8). Two of the soil-heat-flux monitoring locations are located directly below the masts that hold the four-way net radiometers. Additionally, soil temperature is monitored at 496 locations with Decagon 5TM sensors (Figs. 8 and 9). This collection of instruments allows for full accounting of incoming and outgoing short- and long-wave radiation, sensible and latent heat transfer (discussed further in Section 4), and heat transport into the soil. The vertically stratified measurements of temperature and relative humidity above the hillslopes allow quantification of the influence of atmospheric gradients on the net radiation balance at the soil surface.

4. Manipulation and monitoring of the hydrologic cycle at LEO

A custom-engineered irrigation system drives the hydrologic cycle on the LEO landscapes. A sensor network is in place to measure storage and flux components of the terrestrial water balance, as written below

$$\Delta S = P - ET - Q \quad (2)$$

where ΔS is the change in subsurface water storage; P is precipitation; ET is evapotranspiration; Q is discharge, and all variables are functions of time. Each slope is equipped with five independent plumbing circuits with Hunter MP Rotator sprinkler heads installed at 14 equally spaced locations (7 locations on each of the two long sides of the landscapes) sitting ≈3 m above the soil surface. Operating individually, the five circuits produce rainfall rates ranging from 3 to 13 mm h^{-1} that can be applied relatively uniformly over the entire slope or to specific subsections. The maximum rate of 40 mm h^{-1} is achieved when all five circuits operate simultaneously. The distributions of drop sizes and drop velocities produced by the sprinkler heads were measured with a Thies Clima© disdrometer (i.e., a laser precipitation monitor that measures the velocity and drop size of every raindrop). Two examples of these distributions are shown in Fig. 10. The relationship between drop size and terminal velocity (estimated using the empirical equation of Dietrich, 1982) is shown for comparison, demonstrating that the 3- to 4-m fall height (considering the arc of the spray) is sufficient for the drops to achieve velocities close to those of natural rainfall. Complex turbulent interactions between neighboring drops can result in velocities greater than terminal in LEO and in natural rainfall (e.g., Montero-Martinez et al., 2009).

The spatial uniformity of precipitation is greatest for the high-intensity circuits [coefficient of variation (Cv) < 0.2] and becomes more heterogeneous for the low-intensity circuits (Cv as great as 0.70)

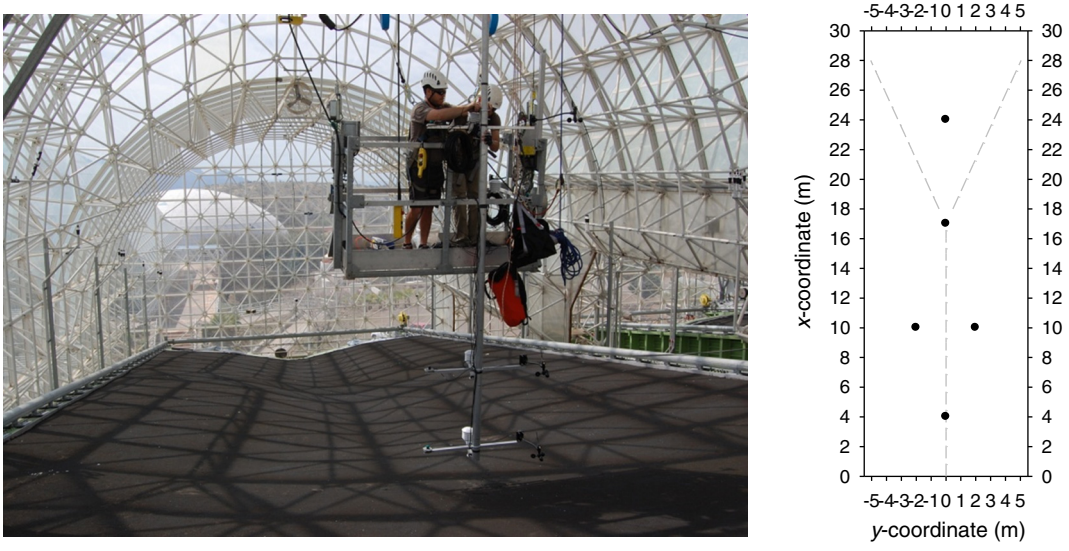

Fig. 7. (left) Photograph of the installation of instruments on one of five vertical masts that hang from the space frame above the LEO landscape. The personnel transport system shown in the picture allows access to any point on the slope without disturbing the landscape surface. Each vertical mast has crossbars located at 0.25, 1, 3, 6, and 9–10 m above the soil surface. Sensors mounted on each crossbar measure temperature, relative humidity, incoming visible light, wind speed and direction, and are equipped with gas sampling ports. (right) Diagram showing the *x*- and *y*-coordinates where vertical masts are located above the landscape surface. The masts located on opposing slopes of the convergence zone (dashed gray line) are also equipped with four-way net radiometers, and the centermost mast is equipped with a three-dimensional sonic anemometer.

Please cite this article as: Pangle, L.A., et al., The Landscape Evolution Observatory: A large-scale controllable infrastructure to study coupled Earth-surface processes, Geomorphology (2015), http://dx.doi.org/10.1016/j.geomorph.2015.01.020

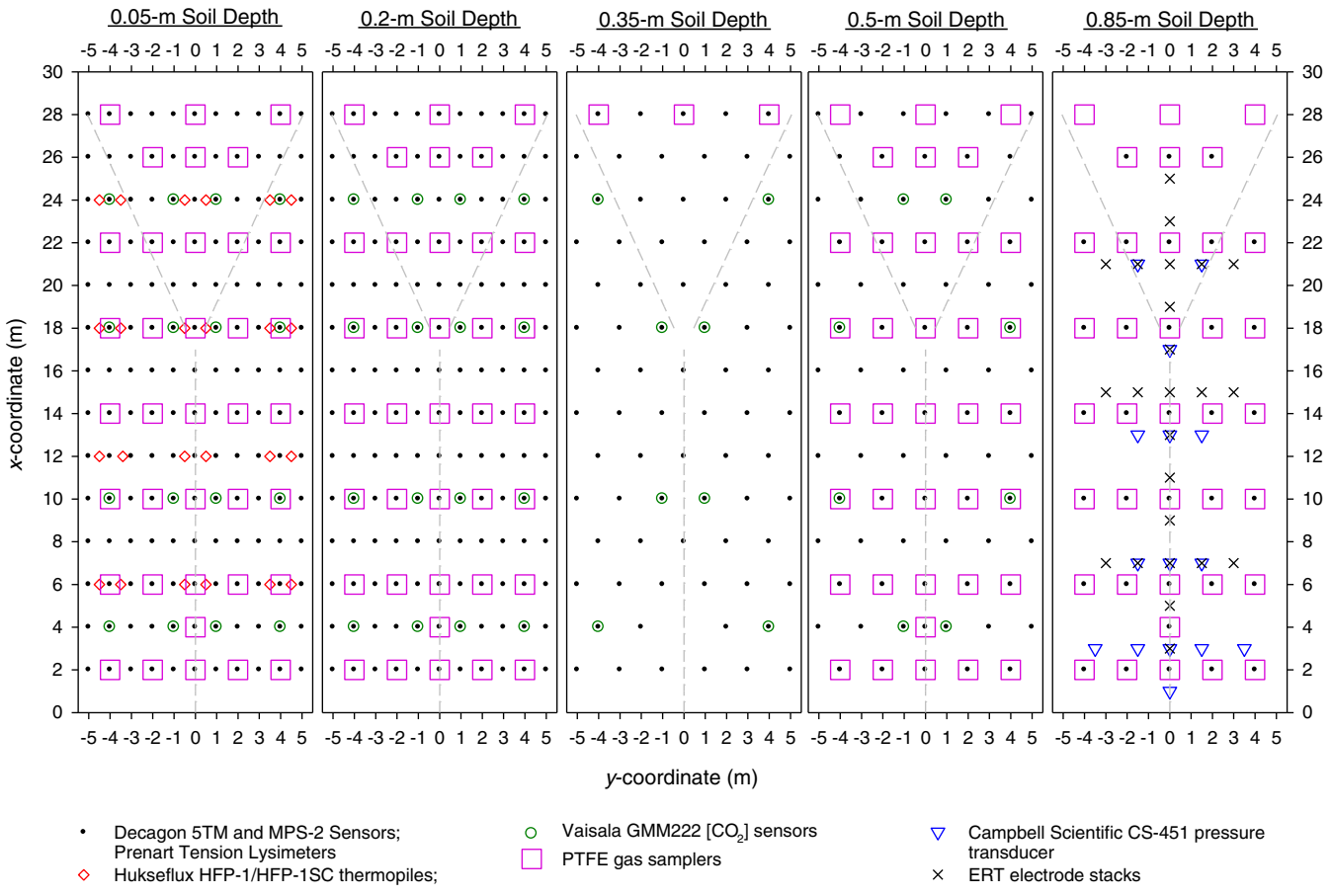

Fig. 8. Diagram showing the lateral and vertical orientation of the sensor/sampler network in the LEO landscapes. Each diagram within the 1 × 5 array represents a specific soil depth (*z*-coordinate), with the depth expressed as a positive distance from the soil surface. Symbol sizes are not drawn to scale, rather to show the *x*, *y*, and *z* location of each sensor. For simplicity, the *x*- and *y*-coordinates of the CS-451 pressure transducers are illustrated on the diagram representing the 0.85-m soil depth, although they are actually located inside bulkhead fittings that are mounted to the base of the steel frame (i.e., soil depth of 1 m). Note that the *x*- and *y*-coordinates for the ERT electrode stacks are illustrated on the same diagram, though the electrodes exist at multiple depths (see details in Section 4 of the text). Dashed gray lines indicate the axial orientation of the zones of convergence.

when considering application over the entire landscape. However, through automatic control of the valves that activate and deactivate each circuit, optimal combinations of the five irrigation circuits can be used to achieve the best possible spatial uniformity (Cv ≈ 0.20) at all rainfall intensities (3–40 mm h^{-1}; see Fig. 11). Depending on the specific rainfall application, some systematic patterning of the rainfall

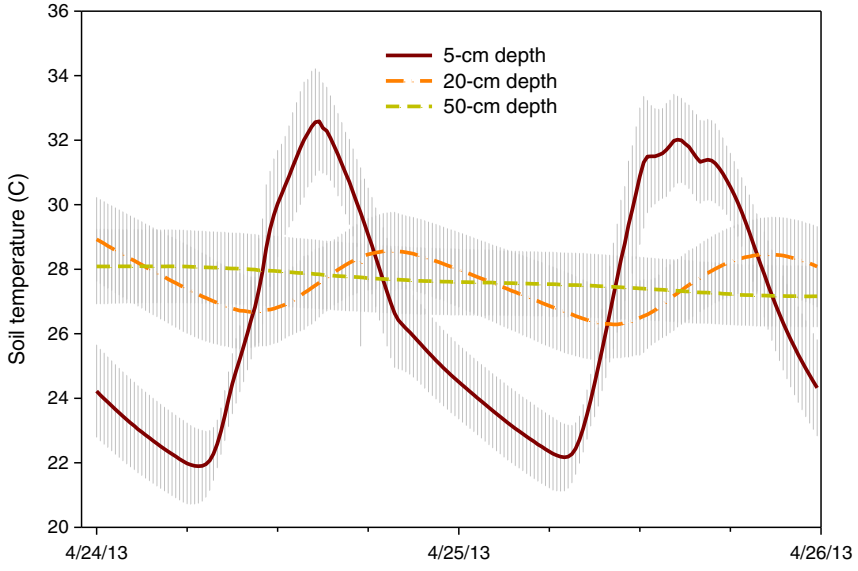

Fig. 9. Two-diel cycles of temperature measured at 5, 20, and 50-cm depths within the crushed basalt that forms the parent material of the LEO landscapes. Error bars indicate the spatial variability among the 154, 154, and 78 probes located at each of those depths, respectively.

Please cite this article as: Pangle, L.A., et al., The Landscape Evolution Observatory: A large-scale controllable infrastructure to study coupled Earth-surface processes, Geomorphology (2015), http://dx.doi.org/10.1016/j.geomorph.2015.01.020

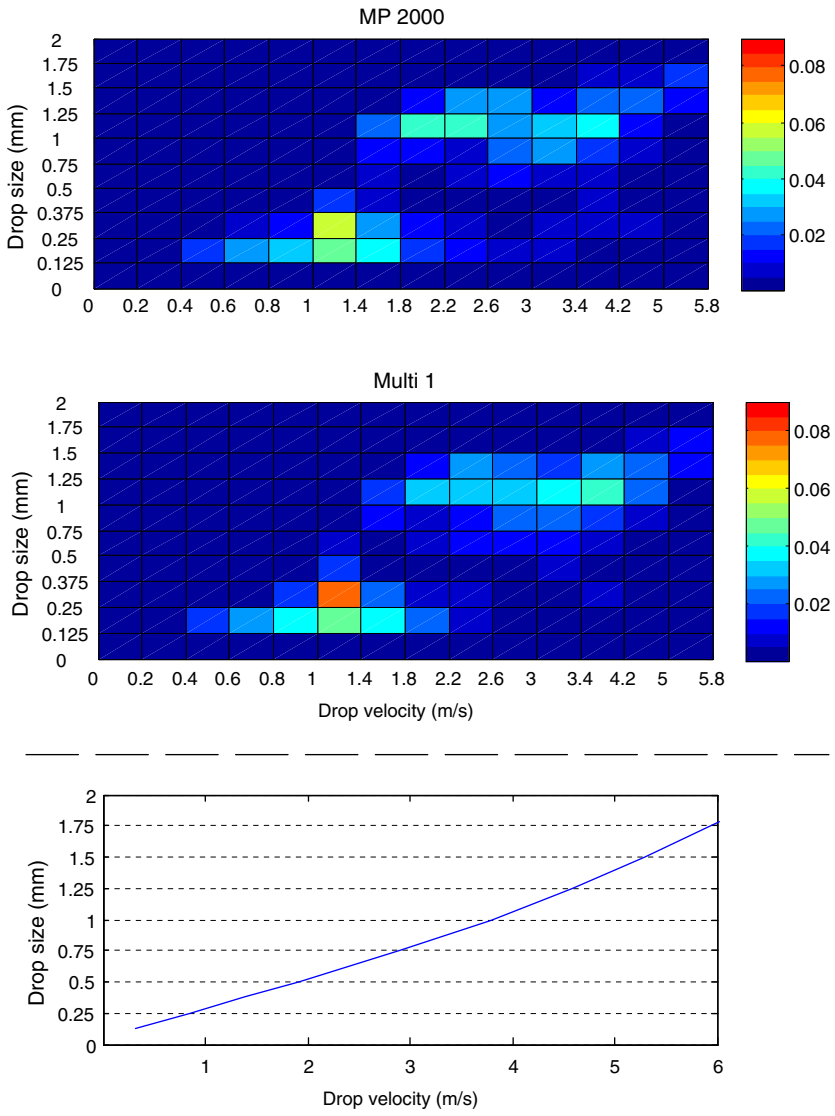

Fig. 10. (top and middle) Color maps illustrating the bivariate frequency distribution (—) of the size and velocity of water drops produced by two of the five individual irrigation circuits. Titles indicate the name of the irrigation circuit. Distributions of drop size and velocity for the other three circuits were very similar, though not shown here. The tick-mark labels on the *x*- and *y*-axes indicate the upper bound of size and velocity bins within which rain drops were grouped. Measurements of drop size and velocity were conducted for each circuit (10 replicate tests per circuit; 5 from upslope, and 5 from downslope positions) using a Thies Clima© disdrometer. (bottom) The relationship between drop velocity and size for natural precipitation, estimated using the empirical equations of Dietrich (1982). (For interpretation of the references to color in this figure legend, the reader is referred to the web version of this article.)

will remain — the potential influence of which can be examined by analysis of the local responses of subsurface sensors. The irrigation water is sourced from a local well, pumped through a reverse osmosis filtration system, and stored temporarily in seven 8000-L tanks (a total storage capacity equivalent to 169 mm of precipitation depth for a single landscape). Replicated sampling over several days indicated that the reverse-osmosis system yields water with an average pH of 7.25 and electrical conductivity of 53.4 μS cm^{-1} (standard deviations of 0.16 and 43.6, respectively). The temperature of the water fluctuates seasonally because of heat transfer in the storage and conveyance system. The tanks have individual valves that facilitate controlled introduction of isotopically labeled precipitation through any of the rainfall circuits in a range of possible spatial or temporal patterns.

Each steel structure and all soil and biomass contained within rest on 10 load cells, making the LEO landscapes three replicates of the largest weighing lysimeter in the world (Fig. 12). Semi-custom Honeywell Model 3130 load cells were designed to maximize measurement capacity and precision. They are specified with a repeatability of ±0.05% of full scale, with hysteresis and nonlinearity at 0.2% full scale. The data-acquisition device adds additional uncertainty of ±0.05% of full scale and ±0.05% reading accuracy error. In addition, 496 soil-water content and temperature sensors (Decagon 5TM sensors, Decagon Devices, Inc.) are buried within each hillslope as follows: 154 sensors are buried at 0.05 and at 0.2-m depth; 76 sensors at 0.35-m depth; 78 sensors at 0.5-m depth; and 34 sensors at 0.85-m depth (Fig. 8). The sensors are located along sampling profiles that are oriented at 90° from the underlying sloping steel structure, providing submeter-scale measurement resolution in the vertical dimension. The horizontal arrangement of these sensors provides 1- to 2-m scale sampling resolution along the short and long axes of the landscapes, respectively, at the 0.05- and 0.2-m depths, with lower total sampling coverage at greater soil depths (Fig. 8). A calibration curve specific to the ground basalt material was developed to convert directly measured dielectric permittivity to values of volumetric water content. This calibration was performed on a total of four sensors. The fitted calibration curve yields 95% confidence intervals around predicted values of volumetric water content that range from ±0.023 to ±0.025. Collectively, the load cells and water content sensors enable unprecedented monitoring of total subsurface water storage and the spatial distribution of that storage through time.

Please cite this article as: Pangle, L.A., et al., The Landscape Evolution Observatory: A large-scale controllable infrastructure to study coupled Earth-surface processes, Geomorphology (2015), http://dx.doi.org/10.1016/j.geomorph.2015.01.020

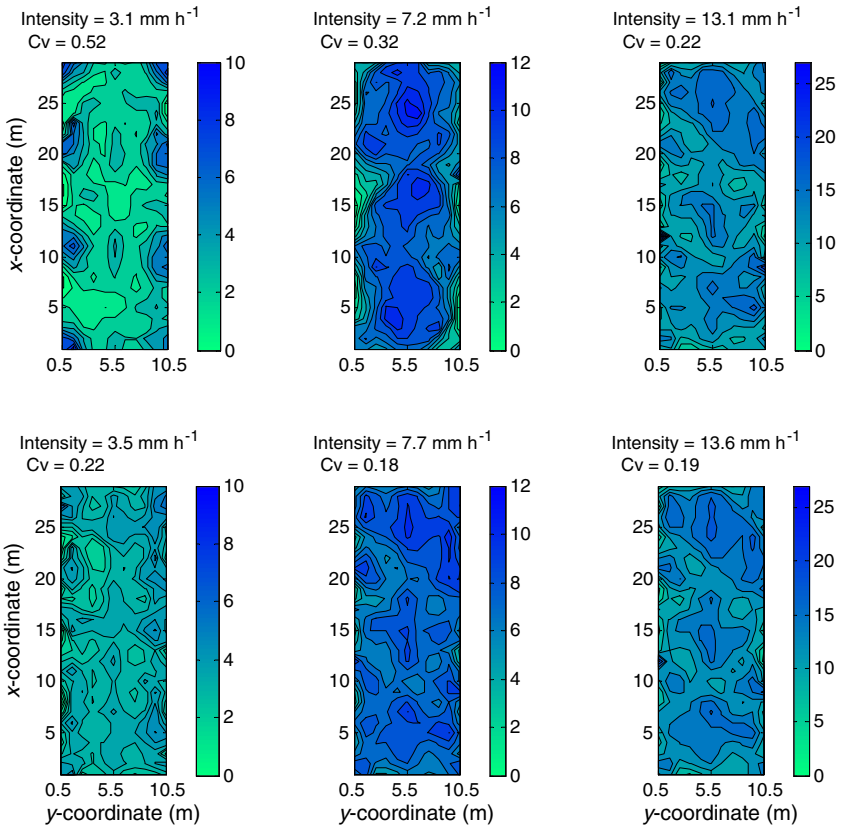

Fig. 11. (upper row) Contour plots illustrating the spatial variability of irrigation applied to the LEO landscapes at varying intensities. Color legend is in mm h^{-1}. For plots in the upper row, the intensity is constant over 1 h, and Cv indicates the coefficient of variation. (lower row) Contour plots illustrating the spatial variability of irrigation when multiple irrigation circuits are used to achieve the best possible spatial uniformity at each level of intensity. For plots in the lower row, the intensity varies over 1 h, depending on the combination of irrigation circuits that are used, but the average intensity is similar to the three cases shown above. The spatial variability of irrigation was measured using timed irrigation trials where 319 cups were spaced in a regular grid on the soil surface to collect and measure the point-scale water accumulation. Contour plots based on these data were created using the *contourf* function in Matlab version 7.10. Note that when all five irrigation circuits are operated simultaneously, the intensity is 40.5 mm h^{-1} and the Cv is 0.18. (For interpretation of the references to color in this figure legend, the reader is referred to the web version of this article.)

The soil-water pressure (i.e., gauge pressure) within the LEO landscapes is monitored at the same spatial and temporal frequency as volumetric water content. Decagon MPS-2 sensors are collocated with the water content sensors at each of 496 sampling locations (Fig. 8). The MPS-2 sensors have a measurement range of −6 to −500 kPa, a manufacturer reported accuracy of ±25% of the measured value, and allow for in situ observation of the water pressure versus water content relationship across very dry to nearly saturated conditions. During saturated conditions, the spatial extent and depth of the saturated zone is estimated with CS451 pressure transducers (Campbell Scientific, Inc.) installed in bulkhead fittings at 15 locations at the interface between the soil profile and the underlying steel structure (Fig. 8). The CS451 pressure transducers measure pressure head across a range of 0 to 2 m. The manufacturer reported accuracy is 0.1% of full-scale range.

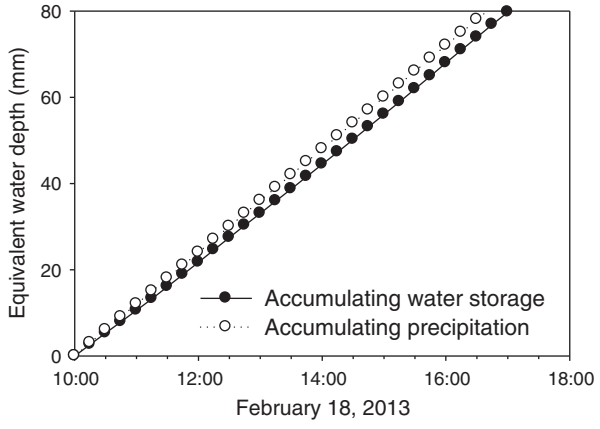

Fig. 12. Time series of accumulating water storage and accumulating precipitation over a 7-hour period on one LEO landscape. The precipitation rate was constant at 12 mm h^{-1}, and no seepage flow occurred during this period. The accumulation of water storage was measured with 10 HoneyWell Model 3130 load cells recording at 15-min intervals.

Custom Prenart SuperQuartz soil-water samplers (Prenart Equipment ApS) are also installed at each of 496 sampling locations; they are connected via Teflon tubing to labeled syringes and enable sampling of soil water for chemical analysis (Fig. 8). The data cables and sample tubing associated with the sensors noted above (and others described in Section 5) are stretched along the sampling profiles within the soil and exit through drilled port holes at the interface between the crushed basalt and the underlying steel structure. The holes are fitted with bulkhead fittings and a short length of acrylic tubing that collates the cable bundle and provides space where a urethane elastomer sealant and expanding foam insulation were used to make a water-tight seal around the cables within the port hole. Inevitably the possibility exists that buried hardware can affect water flow in the subsurface — at LEO or any field site where the same equipment is installed. Despite the great number of devices installed within the LEO landscapes, <1% of the entire landscape volume is actually occupied by any type of hardware. If preferential flow paths develop, and regularly transmit water along the near-vertical profiles of hardware, this phenomenon should be detectable based on comparisons of the timing of response

by water content sensors buried at similar depth across the landscape. Early experiments indicate that the timing of response is remarkably similar among water content sensors buried at the same depth (see Fig. 9 in Gevaert et al., 2014).

Discharge is measured at the seepage-face boundary (11 m^2) at the downslope end of the landscapes. At this boundary, the crushed rock contacts a layer of the basaltic tephra with gravel texture (11-m width × 0.5-m upslope length × 1-m depth) that facilitates rapid drainage of water exuding from the soil. The downslope boundary of the gravel is abutted by a perforated plastic sheet (14% porosity; 0.002-m diameter pores) with steel supports and solid dividers that partition the total area of the seepage face into six sections (Fig. 13). Water flowing out of each section of the seepage face is routed through a magnetic flow meter (SeaMetrics, PE102 Flow Meter; 1% relative error at 0.11–11.4 L min^{-1}) then through a tipping bucket gauge (NovaLynx 26-2501-A Tipping Bucket Gauge). The tipping bucket gauges will undergo repeated calibrations through time to assess any drift in their measurement performance.

Initially the LEO landscapes have a bare surface and the *ET* component of the water balance is comprised solely of evaporation (though vegetation will eventually be introduced on the landscapes; see Section 8). Evaporation is monitored using two independent mass-balance methods. The first method derives the *ET* component of Eq. (2) using measured rates of *P*, *Q*, and Δ*S* (as described above). The second approach to measuring *ET* utilizes instrumentation that is installed on the same vertical masts that were described in Section 3 in a closed-system mass-balance methodology. Each mast holds five anemometers, and the mast that overlies the center of the landscape surface holds a three-dimensional sonic anemometer (CSAT-3; Campbell Scientific, Inc.) that characterizes the wind-velocity field at high temporal resolution. Air intake tubes are installed at each vertical sampling point on all five masts. Air is drawn from the inlet (an inverted B&D Luer-Lock plastic syringe — plunger removed — with a 0.0016-m mesh screen to exclude insects), through 0.0064-m Series 1300 composite tubing (Goodrich Sales, Inc.) to a centrally located 28-position Valco valve (C25G-24528EMT, Valco-VICI), with flow driven by a KNF UN815KNE pump (KNF Neuberger, Inc.; 16 L min^{-1} flow capacity) and directed to a bench-top gas analyzer (LI-7000; LICOR Biosciences, Inc.) for high-precision measurement of [H_2O] and [CO_2] in the air stream. This instrumentation, along with micrometeorological measurements described in Section 3, allows quantification of water vapor storage within the LEO atmosphere, and the time derivative of those measurements provides an estimate of whole-landscape *ET*.

Two final components of the hydrologic monitoring system at LEO are a network of custom electrical resistivity probes and a high-resolution thermal imaging system (HRTI; Infrared Camera Inc. ICI 9640S). Custom five-electrode stacks are installed within the crushed basalt at 24 locations on each landscape (Fig. 8). The data acquisition system includes the Supersting R8 3-dimensional imaging system (AGI Advances Geosciences, Inc.) and specialized software for data processing (RES3DINVx64 software from Geotomo Software). The image sensor of the HRTI has 640 × 480 pixels and will enable measurements at a spatial resolution of 0.5–1 cm^2 depending on the number and orientation of sampling transects. The temperature resolution of the camera is 0.04 °C and it will be mounted on an overhead track system above the LEO hillslopes. The imagery generated by the HRTI, when coupled with atmospheric measurements and known soil properties, will facilitate highly spatially resolved calculations of surface evaporation following methods similar to those applied by Shahraeeni and Or (2010).

5. Measurement of overland flow and topographic changes at LEO

A Leica C10 terrestrial laser scanner will be used to quantify topographic changes caused by diffusive geomorphic processes (e.g., rain splash and bioturbation caused by root growth) and by advective processes such as overland flow. The scanner will be mounted at 2–4 locations on the outside edge of the frame of each tray. Scans from each station will be coregistered using high-resolution scans of Leica targets spaced around the LEO frame. The scanner is capable of a model surface precision of 0.002 m. The Leica Cyclone software will be used to generate a unified point cloud precisely georeferenced to the master coordinate system. Digital elevation models (DEMs) with 1-cm^2 $pixel^{-1}$ resolution will be constructed at regular intervals and following all events with the potential to modify the topography. The laser scanner will also be used to quantify physical attributes (e.g., canopy architectures) of aboveground plant biomass once vegetation is established.

When overland flow is generated, a separate downstream capture and measurement system will be employed. The system is in design phase but, in general, will operate such that water and solid material that reaches the downslope end of the landscapes is captured by thin sheeting that routes it to a separate drainage system before it can percolate through the downslope gravel section. This system will lead to a series of basins with known volume. Fluxes will be measured volumetrically as the basins fill and the relative fluxes of water and mass can be quantified by automated pump sampling, real-time turbidity measurements, and direct measurement of sediment delivery to the basins by gravimetric methods.

6. Monitoring of biological and geochemical components of the LEO carbon cycle

The circulation of carbon between the LEO atmosphere, landscapes, and biological communities is described by the equation below:

$$\Delta C = C_P + C_A + C_W - C_R - C_Q \quad (3)$$

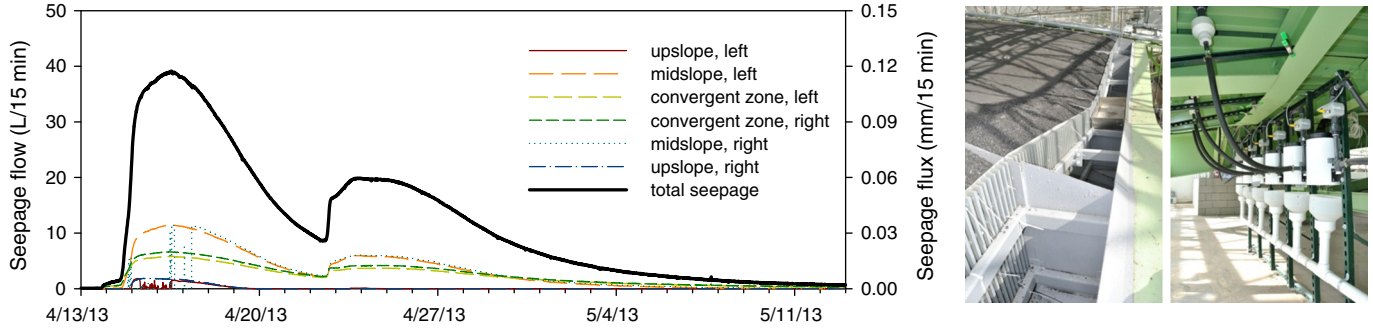

Fig. 13. (left) Time series of seepage from each individual subsection, and the total seepage exiting the landscape during and after three rain pulses applied in April 2013. Note the erratic time series at the upslope, left, and midslope, right locations that occur early in the time series. These data resulted from tipping bucket malfunction and were corrected based on least-squared regression relationships with the seepage data at the upslope, right and midslope, left locations, respectively (R^2 = 0.995 and 0.999, respectively). (right) Photograph of the seepage face boundary at the base of the LEO hillslopes, including the gravel drainage layer, perforated plastic sheet, and the supporting frame that also divides the total seepage face into six subsections. Also, a photograph of the six tipping-bucket gauges and six electromagnetic flow meters that are used to monitor seepage flow from each subsection of the seepage face.

Please cite this article as: Pangle, L.A., et al., The Landscape Evolution Observatory: A large-scale controllable infrastructure to study coupled Earth-surface processes, Geomorphology (2015), http://dx.doi.org/10.1016/j.geomorph.2015.01.020

where ΔC represents the change in carbon storage within the LEO soil and biomass, and the terms on the right-hand side represent time variable fluxes of carbon associated with precipitation inputs (P), gross assimilation through photosynthesis (A) and geochemical weathering reactions (W), ecosystem respiration (R), and carbon exports in discharge (Q).

The same three-dimensional sonic anemometer, gas analyzer, and distributed vertical profiles of gas intake ports described in Section 4 are used to measure the CO_2 storage in the LEO atmosphere over time. The time derivative of this data series provides an estimate of net-ecosystem exchange (i.e., the difference $C_A - C_R$ in Eq. (3)) over the LEO landscapes given the condition of control-volume closure from the external environment. Overnight these gas exchange measurements provide a direct estimate of whole-ecosystem respiration, the magnitude of which can be added to daytime net ecosystem exchange measurements to approximate gross photosynthesis [C_A in Eq. (3)].

High spatial- and spectral-resolution visible to near infrared (VNIR) imaging systems will be installed above each landscape during the winter/spring of 2014/2015. These imaging systems will support analyses of the relationship between chlorophyll fluorescence and C_A across the LEO landscapes. The proposed spectral range of the camera is ≈400–1075 nm over 128 bands, with a spectral resolution of <5 nm (the optimal model and specifications are currently being reviewed prior to purchase). The VNIR imaging system will be mounted in series with the HRTI camera on an automated track system (MSA-14S; Misumi USA, Inc.) that enables linear-position accuracy of 0.001 m. The track system will be suspended from the Biosphere 2 space frame at ≈7.5 m above the soil surface and will enable repeated measurements along a transect spanning the long axes of the landscapes. Both cameras will be contained within environmentally controlled Pelican cases with viewing windows that do not interfere with spectral measurements. The anticipated field of view projected by the lens will cover half the width of the landscape and the anticipated spatial resolution for spectral measurements will be ≈1 cm^2. There have been significant recent advances in understanding of how passive fluorescence measurements can be utilized to estimate photosynthetic carbon assimilation (e.g., Meroni et al., 2009), and recent analyses have demonstrated the utility of these measurements for estimating gross photosynthesis over large spatial scales (e.g., Frankenberg et al., 2011). The radiation environment within the LEO facility may present unique challenges to accurately correlate fluorescence measurements with C_A, although LEO offers the advantage that any such C_A estimates will be very well constrained because of the direct measurement of the other components of the closed-system carbon cycle [Eq. (3)].

The storage, transformation, and flux of carbon in the liquid, solid, and gas phases are monitored within the LEO soil. The extensive network of suction lysimeters enables sampling of the soil-liquid phase, and an on-site analytical laboratory is available for measurement of dissolved organic and inorganic forms of carbon. Similarly, custom-made autosampling devices are in place to collect samples of discharge when it is generated. Forty-eight [CO_2] sensors (Vaisala CARBOCAP GMM220) are installed in the LEO soil (Fig. 8) for continuous automated monitoring of the [CO_2] in the soil-gas phase. To extract discrete samples of soil gas for chemical analysis, 151 custom made gas-sampling tubes were installed in the soil (Fig. 8). The tubes are constructed from 0.3-m length and 0.0064-m diameter microporous Teflon tubing with pore sizes ranging from 10 to 35 μm, yielding a total porosity of 50% (Zeus Industrial Products). That tubing covers pre-drilled sections of 0.0032-m diameter Teflon tubing (Parker 103-0125031-NT-1000, Controlled Motion Solutions) that are sealed together with epoxy and heat shrink tubing. The exchange loop in the soil is 0.3 m long and total length is 14 m. Gas-phase sampling for isotope analysis is accomplished by using a flow-through loop that allows continuous measurement, via laser spectroscopy, of the same gas volume for sufficient time to allow the measurement to equilibrate.

Monitoring of biological and geochemical components of the carbon cycle at LEO will also include periodic destructive soil sampling for chemical analysis and physiological measurements performed on individual plants. These tasks can be performed without walking on the LEO landscapes through the use of a personnel transport system (Tractel, Inc.; shown in Figs. 2 and 7).

7. Acquisition and storage of LEO data and dissemination to the scientific community

All sensor types (whether digital, analog, or pulse-generating devices) transmit to one of four compact reconfigurable control and acquisition systems (National Instruments CompactRIO; model cRIO-9074), with modules that serve as input/output devices (or both) or as a communications bus. Analog devices are continuously sampled and the cRIO is programmed to perform basic signal processing (e.g., moving averages). In total, there are 992 Decagon sensors (MPS-2 and 5TM) that use the SDI-12 communication protocol and interface with the cRIOs via a custom breakout board. All other recording instruments connect directly to modules within the cRIOs. The cRIOs are programmed to store ≈30 days of data from the entire hillslope monitoring system. This provides resilience during any periods of network outage.

Data storage and dissemination occur on two servers located at Biosphere 2. Text files (i.e., current state files) are sent to a data-acquisition server that parses the text, extracts data, and uploads to the database server. The data acquisition server allows real-time monitoring of all data streams, whereas the two functions of the database server are to archive data and enable visualization and publishing. The LEO database (SensorDB) adopted the control vocabulary from the Observations Data Model (ODM; see Horsburgh et al., 2008). The data model used for LEO was developed and implemented as a relational database. It focuses on the extensive description of sensors (metadata), allowing simplified reporting of each value of time, sensor, and variable.

LEO was intended to be a tool for the scientific community. Researchers that have interests in performing experiments at LEO are encouraged to contact Biosphere 2 affiliates to discuss potential collaborative opportunities. Live data streams from LEO can be viewed at http://b2.arizona.edu:8080/LEOdatasets. At that URL, researchers can also find the contact information needed to request access to the database, data-use policies, and metadata. The webpage interface allows querying of the data based on sensor type, sensor location within the landscape, variable (for sensors reporting multiple variables), and time.

8. The operational model for collaborative observational and experimental research at LEO

LEO is a community-planned research infrastructure aimed at advancing our knowledge of coupled Earth-surface processes through collaborative and interdisciplinary research. To achieve that goal, a scientific plan was developed that includes a long-term experiment focused on intensive monitoring and modeling of the coevolution of soil, landscape morphology, biological communities, and mass and energy exchange processes under controlled climate conditions. Within that long-term study period, there are further opportunities for shorter term manipulative experiments, with the goal of fostering diverse modes of experimental and theoretical research that span time scales of days to years.

The model for research at LEO includes a multiyear period of monitoring and experimentation during which each landscape receives the same regime of temperature, humidity, and precipitation. The initiation of that climate regime will commence once the final installation of meteorological and gas-sampling equipment over the central and west landscapes is complete. It is most economical to operate LEO such that air temperature is within 5 °C of ambient temperature outside

Please cite this article as: Pangle, L.A., et al., The Landscape Evolution Observatory: A large-scale controllable infrastructure to study coupled Earth-surface processes, Geomorphology (2015), http://dx.doi.org/10.1016/j.geomorph.2015.01.020

of Biosphere 2, although it is logistically possible to deviate substantially from those conditions for extended experimental periods. Thus, seasonal variation in air temperature will most often follow trends typical of Sonoran Desert uplands. This long-term climate-control plan, combined with shorter term experimental climate manipulations, allows for significant flexibility so that landscape evolution, energy, water, and carbon cycling processes can be studied under a broad range of conditions in a relatively short amount of time (i.e., several years).

The precipitation regime will include sequences of rainfall events applied during warm and cold seasons, followed by extended drought periods. This regime acknowledges that the impact of water availability on Earth-surface processes across different bioclimatic settings can be best investigated by creating significant variation in water inputs across a range of temperature conditions. Data from LEO will have relevance to systems like the Sonoran Desert, where frontal systems cause relatively low-intensity storms during the North American winter season, and localized convective storms generate high-intensity rainfall during the summer monsoon season. Variation in water inputs and temperature should also be sufficient to be relevant to the winter/spring driven Mojave Desert and the summer-intensive growing season in the Chihuahuan Desert. Similar to the temperature and relative humidity regimes, there will be flexibility in the amounts of rainfall applied during cold and warm seasons within LEO, and among years, to accommodate diverse research objectives.

The introduction of vascular plant species onto the LEO landscapes provides another opportunity (similar to the original LEO planning phase) to openly engage the broader scientific community through planning workshops. These forthcoming workshops will be aimed at identifying important contemporary research questions in community and physiological ecology that could be uniquely addressed at LEO. Preliminary tests are underway to determine how well various plant species will germinate and grow on the crushed basalt. These data will provide baseline information to guide that community-based decision making process.

Sterilization of the LEO soil was not feasible because of the immense volume, although the extremely small amounts of organic carbon (Table 1) in the crushed basalt suggest minimal presence of life. Samples of the original material are currently being analyzed using DNA sequencing techniques to quantify the microbial diversity existing within the ground basalt in its initial state. This effort is led by an interdisciplinary team of scientists from the University of Arizona and the National Autonomous University of Mexico.

The control over climate variables at LEO is planned with significant flexibility so that shorter term experiments may be executed within the longer term climate simulation. These shorter term experiments represent another opportunity for community involvement. Two short-term studies were conducted during February and April 2013 that used rainfall applications, stable-isotope tracers, and numerical modeling to investigate hydrological processes and incipient spatial differentiation of soil properties on one LEO landscape (Gevaert et al., 2014; Niu et al., 2014). These collaborative works involved researchers from institutions in the USA, Canada, Italy, and the Netherlands, and benchmarked some early aspects of the hydrology of the LEO landscapes that will be used to detect change over time. These early works also illustrate the iterative scientific approach that can be uniquely performed at LEO; that is, numerical-model simulation, actual physical experimentation, and learning through combined data analysis and retrospective analysis of model parameters. Short-term dedicated experiments like these may require intensive use of the sampler network and associated laboratory analyses that exceed the sampling and analysis frequencies associated with the long-term observational study of landscape evolution processes. As such, potential collaborators are encouraged to contact University of Arizona affiliates to discuss opportunities for proposal development and funding acquisition to support these experiments. That contact information can be found at the Biosphere 2 website.

9. Conclusion

The Landscape Evolution Observatory was conceived through a community-based planning process as an innovative research infrastructure for investigating coupled water, carbon, and energy cycling under simulated climate conditions and during landscape evolution (Huxman et al., 2009). The facility is now operational, though its measurement capability continues to be developed and improved. LEO enables an unequaled level of environmental control over a spatial scale approaching those included in many observational field studies, and in a system that is replicated. LEO is operated by the University of Arizona but is envisioned as a tool that can be utilized by the broader Earth-science community. As such, automated data are made available online in real time, and collaboration from investigators external to the University of Arizona is encouraged. The LEO science plan includes an adaptive trajectory of detailed observation and controlled experimentation during a 10-year period of landscape evolution. This plan will accommodate the need to carefully measure long-term changes in landscape form and function and the need for short-term manipulative experimentation.

Acknowledgments

The Biosphere 2 facility and the capital required to conceive and construct LEO were provided through a charitable donation from the Philecology Foundation, and its founder, Mr. Edward Bass. We gratefully acknowledge that charitable donation. LEO was conceived through a community planning effort that included intellectual contributions from many scientists from the USA and other nations. The board of advisors provided a series of design and plan review exercises that significantly improved the direction and final outcome of LEO. Early planning workshops were also supported through the NSF-funded Hydrologic Synthesis Project: Water Cycle Dynamics in a Changing Environment: Advancing Hydrologic Science Through Synthesis; NSF Grant EAR-0636043, PI: Murugesu Sivapalan. We gratefully acknowledge the collaborative design and construction process that occurred over a nearly three-year period and included the University of Arizona, M3 Engineering, and Lloyd Construction LLC. We particularly thank A. Ortega and D. Mulligan (M3); R. Skinner, F. Ferro, and J. Stiers (Lloyd Construction); T. Parsons, T. Glenn, and J. Glenn (Parsons Steel Erectors); C. Gadjorus (UA Planning and Development), and a long list of highly adaptable and collaborative subcontractors and suppliers too numerous to name. Photos and video from the construction of LEO are available at the Biosphere 2 website. Acquisition of the automated track systems and the imaging systems was supported by NSF Grant EAR-1340912. Additional funding support was provided by the Water, Environmental, and Energy Solutions (WEES) initiative at the University of Arizona and by the Office of the Vice President of Research at the University of Arizona. These funding sources are gratefully acknowledged.

References

Adams, H.D., Guardiola-Claramonte, M., Barron-Gafford, G.A., Villegas, J.C., Breshears, D.D., Zou, C.B., Troch, P.A., Huxman, T.E., 2009. Temperature sensitivity of drought-induced tree mortality portends increased regional die-off under global-change-type drought. Proc. Natl. Acad. Sci. U. S. A. 106, 7063–7066.

Ali, G., Tetzlaff, D., Soulsby, C., McDonnell, J.J., 2012a. Topographic, pedologic and climatic interactions influencing streamflow generation at multiple catchment scales. Hydrol. Process. 26, 3858–3874.

Ali, G., Tetzlaff, D., Soulsby, C., McDonnell, J.J., Capell, R., 2012b. A comparison of similarity indices for catchment classification using a cross-regional dataset. Adv. Water Resour. 40, 11–22.

Angers, D.A., Caron, J., 1998. Plant-induced changes in soil structure: processes and feedbacks. Biogeochemistry 42, 55–72.

Please cite this article as: Pangle, L.A., et al., The Landscape Evolution Observatory: A large-scale controllable infrastructure to study coupled Earth-surface processes, Geomorphology (2015), http://dx.doi.org/10.1016/j.geomorph.2015.01.020

Bachmair, S., Weiler, M., 2012. Hillslope characteristics as controls of subsurface flow variability. Hydrol. Earth Syst. Sci. 16, 3699–3715.

Bachmair, S., Weiler, M., Troch, P.A., 2012. Intercomparing hillslope hydrological dynamics: spatio-temporal variability and vegetation cover effects. Water Resour. Res. 48, W05537.

Beven, K., 2012. Causal models as multiple working hypotheses about environmental processes. Compt. Rendus Geosci. 344, 77–88.

Brantley, S.L., Goldhaber, M.B., Ragnarsdottir, K.V., 2007. Crossing disciplines and scales to understand the critical zone. Elements 3, 307–314.

Bromley, J., Brouwer, J., Barker, A.P., Gaze, S.R., Valentin, C., 1997. The role of surface water redistribution in an area of patterned vegetation in a semi-arid environment, south-west Niger. J. Hydrol. 198, 1–29.

Chorover, J., Kretzschmar, R., Garcia-Pichel, F., Sparks, D.L., 2007. Soil biogeochemical processes within the critical zone. Elements 3, 321–326.

Chorover, J., Troch, P.A., Rasmussen, C., Brooks, P.D., Pelletier, J.D., Breshears, D.D., Huxman, T.E., Kurc, S.A., Lohse, K.A., McIntosh, J.C., Meixner, T., Schaap, M.G., Litvak, M.E., Perdrial, J., Harpold, A., Durcik, M., 2011. How water, carbon, and energy drive critical zone evolution: the Jemez–Santa Catalina Critical Zone Observatory. Vadose Zone J. 10, 884–899.

Clark, M.P., Kavetski, D., Fenicia, F., 2011. Pursuing the method of multiple working hypotheses for hydrological modeling. Water Resour. Res. 47, W09301.

Dietrich, W.E., 1982. Settling velocity of natural particles. Water Resour. Res. 18, 1615–1626.

Dietrich, W.E., Reneau, S.L., Wilson, C.J., 1987. Overview: "zero-order basins" and problems of drainage density, sediment transport and hillslope morphology. Int. Assoc. Hydrol. Sci. Bull. 165, 27–37.

Dietrich, W.E., Wilson, C.J., Montgomery, D.R., McKean, J., Bauer, R., 1992. Erosion thresholds and land surface-morphology. Geology 20, 675–679.

Dietrich, W.E., Reiss, R., Hsu, M.L., Montgomery, D.R., 1995. A process-based model for colluvial soil depth and shallow landsliding using digital elevation data. Hydrol. Process. 9, 383–400.

Dontsova, K., Steefel, C.I., Desilets, S., Thompson, A., Chorover, J., 2009. Solid phase evolution in the Biosphere 2 hillslope experiment as predicted by modeling of hydrologic and geochemical fluxes. Hydrol. Earth Syst. Sci. 13, 2273–2286.

Dunne, T., Malmon, D.V., Mudd, S.M., 2010. A rain splash transport equation assimilating field and laboratory measurements. J. Geophys. Res. Earth Surf. 115, F01001.

Dybas, C., 2013. Discoveries in the Critical Zone: Where Life Meets Rock. National Science Foundation Discovery Articles.

Fenicia, F., McDonnell, J.J., Savenije, H.H.G., 2008. Learning from model improvement: on the contribution of complementary data to process understanding. Water Resour. Res. 44, W06419.

Finn, M., 1996. The mangrove mesocosm of Biosphere 2: design, establishment and preliminary results. Ecol. Eng. 6, 21–56.

Frankenberg, C., Fisher, J.B., Worden, J., Badgley, G., Saatchi, S.S., Lee, J.-E., Toon, G.C., Butz, A., Jung, M., Kuze, A., Yokota, T., 2011. New global observations of the terrestrial carbon cycle from GOSAT: patterns of plant fluorescence with gross primary productivity. Geophys. Res. Lett. 38, L17706.

Freer, J., McDonnell, J.J., Beven, K.J., Peters, N.E., Burns, D.A., Hooper, R.P., Aulenbach, B., Kendall, C., 2002. The role of bedrock topography on subsurface storm flow. Water Resour. Res. 38, 1269.

Gevaert, A.I., Teuling, A.J., Uijlenhoet, R., DeLong, S.B., Huxman, T.E., Pangle, L.A., Breshears, D.D., Chorover, J., Pelletier, J.D., Saleska, S.R., Zeng, X., Troch, P.A., 2014. Hillslope-scale experiment demonstrates the role of convergence during two-step saturation. Hydrol. Earth Syst. Sci. 18, 3681–3692.

Harman, C.J., Lohse, K.A., Troch, P.A., Sivapalan, M., 2014. Spatial patterns of vegetation, soils, and microtopography from terrestrial laser scanning on two semiarid hillslopes of contrasting lithology. J. Geophys. Res. Biogeosci. 119, 163–180.

Hopp, L., Harman, C., Desilets, S.L.E., Graham, C.B., McDonnell, J.J., Troch, P.A., 2009. Hillslope hydrology under glass: confronting fundamental questions of soil–water–biota co-evolution at Biosphere 2. Hydrol. Earth Syst. Sci. 13, 2105–2118.

Horsburgh, J.S., Tarboton, D.G., Maidment, D.R., Zaslavsky, I., 2008. A relational model for environmental and water resources data. Water Resour. Res. 44, W05406.

Hurlbert, S.H., 1984. Pseudoreplication and the design of ecological field experiments. Ecol. Monogr. 54, 187–211.

Huxman, T.E., Troch, P.A., Chorover, J., Breshears, D.D., Saleska, S., Pelletier, J., Zeng, X., Espeleta, J., 2009. The hills are alive: Earth science in a controlled environment. EOS Trans. Am. Geophys. Union 90.

Ivanov, V.Y., Fatichi, S., Jenerette, G.D., Espeleta, J.F., Troch, P.A., Huxman, T.E., 2010. Hysteresis of soil moisture spatial heterogeneity and the "homogenizing" effect of vegetation. Water Resour. Res. 46, W09521.

Jenerette, G.D., Shen, W., 2012. Experimental landscape ecology. Landsc. Ecol. 27, 1237–1248.

Kirchner, J.W., 2006. Getting the right answers for the right reasons: linking measurements, analyses, and models to advance the science of hydrology. Water Resour. Res. 42, W03S04.

Kleinhans, M.G., Bierkens, M.F.P., van der Perk, M., 2010. HESS opinions on the use of laboratory experimentation: 'hydrologists, bring out shovels and garden hoses and hit the dirt'. Hydrol. Earth Syst. Sci. 14, 369–382.

Marino, B.D.V., Mahato, T.R., Druitt, J.W., Leigh, L., Lin, G., Russell, R.M., Tubiello, F.N., 1999. The agricultural biome of Biosphere 2: structure, composition and function. Ecol. Eng. 13, 199–234.

McGrath, G.S., Hinz, C., Sivapalan, M., 2007. Temporal dynamics of hydrological threshold events. Hydrol. Earth Syst. Sci. 11, 923–938.

Meroni, M., Rossini, M., Guanter, L., Alonso, L., Rascher, U., Colombo, R., Moreno, J., 2009. Remote sensing of solar-induced chlorophyll fluorescence: review of methods and applications. Remote Sens. Environ. 113, 2037–2051.

Montero-Martinez, G., Kostinski, A.B., Shaw, R.A., Garcia-Garcia, F., 2009. Do all raindrops fall at terminal speed? Geophys. Res. Lett. 36, L11818.

Montgomery, D.R., Dietrich, W.E., Torres, R., Anderson, S.P., Heffner, J.T., 1997. Hydrologic response of a steep unchanneled valley to natural and applied rainfall. Water Resour. Res. 33, 91–109.

Niemann, J.D., Hasbargen, L.E., 2005. A comparison of experimental and natural drainage basin morphology across a range of scales. J. Geophys. Res. Earth Surf. 110, F04017.

Niu, G.-Y., Pasetto, D., Scudeler, C., Paniconi, C., Putti, M., Troch, P.A., DeLong, S.B., Dontsova, K., Pangle, L., Breshears, D.D., Chorover, J., Huxman, T.E., Pelletier, J., Saleska, S., Zeng, X., 2014. Incipient subsurface heterogeneity and its effect on overland flow generation — insight from a modeling study of the first experiment at the Biosphere 2 Landscape Evolution Observatory. Hydrol. Earth Syst. Sci. 18, 1873–1883.

Norby, R.J., Luo, Y.Q., 2004. Evaluating ecosystem responses to rising atmospheric CO_2 and global warming in a multi-factor world. New Phytol. 162, 281–293.

Norby, R.J., Zak, D.R., 2011. Ecological lessons from free-air CO_2 enrichment (FACE) experiments. Annu. Rev. Ecol. Evol. Syst. 42, 181–203.

Osmond, B., Ananyev, G., Berry, J., Langdon, C., Kolber, Z., Lin, G.H., Monson, R., Nichol, C., Rascher, U., Schurr, U., Smith, S., Yakir, D., 2004. Changing the way we think about global change research: scaling up in experimental ecosystem science. Glob. Chang. Biol. 10, 393–407.

Pelletier, J.D., Barron-Gafford, G.A., Breshears, D.D., Brooks, P.D., Chorover, J., Durcik, M., Harman, C.J., Huxman, T.E., Lohse, K.A., Lybrand, R., Meixner, T., McIntosh, J.C., Papuga, S.A., Rasmussen, C., Schaap, M., Swetnam, T.L., Troch, P.A., 2013. Coevolution of nonlinear trends in vegetation, soils, and topography with elevation and slope aspect: a case study in the sky islands of southern Arizona. J. Geophys. Res. Earth Surf. 118, 741–758.

Phillips, J.D., 2003. Sources of nonlinearity and complexity in geomorphic systems. Prog. Phys. Geogr. 27, 1–23.

Rasmussen, C., Troch, P.A., Chorover, J., Brooks, P., Pelletier, J., Huxman, T.E., 2011. An open system framework for integrating critical zone structure and function. Biogeochemistry 102, 15–29.

Saco, P.M., Willgoose, G.R., Hancock, G.R., 2007. Eco-geomorphology of banded vegetation patterns in arid and semi-arid regions. Hydrol. Earth Syst. Sci. 11, 1717–1730.

Shahraeeni, E., Or, D., 2010. Thermo-evaporative fluxes from heterogeneous porous surfaces resolved by infrared thermography. Water Resour. Res. 46, W09511.

Sidle, R.C., Tsuboyama, Y., Noguchi, S., Hosoda, I., Fujieda, M., Shimizu, T., 2000. Stormflow generation in steep forested headwaters: a linked hydrogeomorphic paradigm. Hydrol. Process. 14, 369–385.

Stavi, I., Lavee, H., Ungar, E.D., Sarah, P., 2009. Ecogeomorphic feedbacks in semiarid rangelands: a review. Pedosphere 19, 217–229.

Thompson, S.E., Harman, C.J., Heine, P., Katul, G.G., 2010. Vegetation–infiltration relationships across climatic and soil type gradients. J. Geophys. Res. Biogeosci. 115, G02023.

Thompson, S.E., Harman, C.J., Troch, P.A., Brooks, P.D., Sivapalan, M., 2011. Spatial scale dependence of ecohydrologically mediated water balance partitioning: a synthesis framework for catchment ecohydrology. Water Resour. Res. 47, W00J03.

Troch, P.A., Carrillo, G., Sivapalan, M., Wagener, T., Sawicz, K., 2013. Climate–vegetation–soil interactions and long-term hydrologic partitioning: signatures of catchment co-evolution. Hydrol. Earth Syst. Sci. 17, 2209–2217.

Underwood, A.J., 1993. The mechanics of spatially replicated sampling programs to detect environmental impacts in a variable world. Aust. J. Ecol. 18, 99–116.

Vache, K.B., McDonnell, J.J., 2006. A process-based rejectionist framework for evaluating catchment runoff model structure. Water Resour. Res. 42, W02409.

van Tol, J.J., Le Roux, P.A.L., Hensley, M., 2010a. Soil indicators of hillslope hydrology in the Bedford catchments, South Africa. South African J. Plant Soil 27, 242–251.

van Tol, J.J., le Roux, P.A.L., Hensley, M., Lorentz, S.A., 2010b. Soil as indicator of hillslope hydrological behaviour in the Weatherley Catchment, Eastern Cape, South Africa. Water SA 36, 513–520.

Wilson, C.J., Dietrich, W.E., 1987. The contribution of bedrock groundwater flow to storm runoff and high pore pressure development in hollows. Proceedings of the International Symposium on Erosion and Sedimentation in the Pacific Rim, 3–7 August, 1987, Corvallis, Oregon, USA. Int. Assoc. Hydrol. Sci. Bull. 165, 49–59.

Zehe, E., Fluhler, H., 2001. Preferential transport of isoproturon at a plot scale and a field scale tile-drained site. J. Hydrol. 247, 100–115.

Zehe, E., Sivapalan, M., 2009. Threshold behaviour in hydrological systems as (human) geo-ecosystems: manifestations, controls, implications. Hydrol. Earth Syst. Sci. 13, 1273–1297.

Please cite this article as: Pangle, L.A., et al., The Landscape Evolution Observatory: A large-scale controllable infrastructure to study coupled Earth-surface processes, Geomorphology (2015), http://dx.doi.org/10.1016/j.geomorph.2015.01.020